Neutral hydrogen in a region of Cepheus - Nearby galactic structure

Simonson III, S.C.; Someren Greve, H.W. van

Astron. & Astrophys. 49, 343—356 (1976)

Neutral Hydrogen in a Region of Cepheus: Nearby Galactic Structure

S. Christian Simonson, III
University of Maryland

H. W. van Someren Greve
Sterrewacht, Leiden

Received September 29, 1975

Summary. The region $\ell=90°$ to $115°$, $b=-1°$ to $+15°$, was surveyed in the 21-cm line at Dwingeloo. Several correlations were found between H I concentrations and young optical features. An H I self-absorption feature coincides with a line of small, opaque dust clouds and a few Orion-population variables in Khavtassi 141 ($\ell=92°$, $b=+2°$). An H I concentration at $\ell=110°$, $b=+13°$, $V=-9\ \mathrm{km\ s^{-1}}$, also contains a number of Orion-population variables at a distance of 400 pc. These two features connect with other H I extending to $\ell\approx 170°$ at $b\approx +10°$. The velocity pattern resembles material behind a shock with a pitch angle $\approx 20°$ and peculiar inward velocity of $10\ \mathrm{km\ s^{-1}}$. At ~ 800 pc from the sun, two concentrations of H I were found in the vicinity of Cep OB2 and OB3. A large H I shell, 8° in diameter, comprising $5.3\times 10^4\ \mathcal{M}_\odot$ of H I expanding at $10\ \mathrm{km\ s^{-1}}$ and coinciding with a ring of dark clouds, surrounds Cep OB3. The H II region CTB 107 appears to belong to this group. An older and a younger stellar subgroup are found in Cep OB2. An H I concentration was found around the H II region IC 1396 in the younger subgroup. Sub-concentrations coincide with bright-rimmed dark clouds. The region of the older subgroup was found to have low H I content but significant ionization, in accordance with the stellar uv.

Key words: galactic structure — interstellar matter — 21-cm radiation — dust — star clusters and associations

1. Introduction

The region in Cepheus between $\ell=90°$ and $115°$, $b=-1°$ and $+15°$, contains a variety of young stellar features near the sun associated with gas and dust. Cep OB2 and OB3 lie here at distances $R\approx 800$ pc. Star formation has been in progress for 10^7 years in these associations. Closer to the sun, at $R\approx 400$ pc, are the cluster of infrared stars in NGC 7023, the reflection nebula association Cep R2, and a number of Orion-population variables. Here star formation is apparently occurring now. The region offers the opportunity of studying the relationship between stars, dust, and gas where large-scale star formation has been going on. The features are near enough so that the important neutral hydrogen structures can be studied with a radio telescope of moderate size.

Simonson (1968), using the Kootwijk survey, made an earlier comparison of the stellar distribution and the neutral hydrogen distribution. He found concentrations of H I in the vicinity of Cep OB2 and Cep OB3. The present 21-cm line observations were made to investigate this further, using the higher resolution in angle and velocity afforded by the Dwingeloo instrument. Additional stellar observations have been published since the earlier work, allowing a more thorough comparison. In the present study several distinct regions are identified that show a significant correlation between neutral hydrogen features and optical features, both stars and dust. These regions are discussed individually in Sections 4–8. The results are interpreted as indications of the history of the region. Some tentative conclusions are drawn about the effects of star formation on the structure of the interstellar medium during the development of stellar associations. Some consequences for the observational basis of the theory of spiral density waves are pointed out.

2. Observations

a) *The* 21-cm H I *Observations*

The observations were made between June 1968 and September 1969 with the Dwingeloo 25-m radio telescope (beamwidth 0°.61 × 0°.66) with a bandwidth of 8 kHz ($1.7\ \mathrm{km\ s^{-1}}$). The standard reduction procedure was followed (Burton, 1970). The positions of these measurements are given in Fig. 1. The H I line profile was observed at each position over a velocity range from

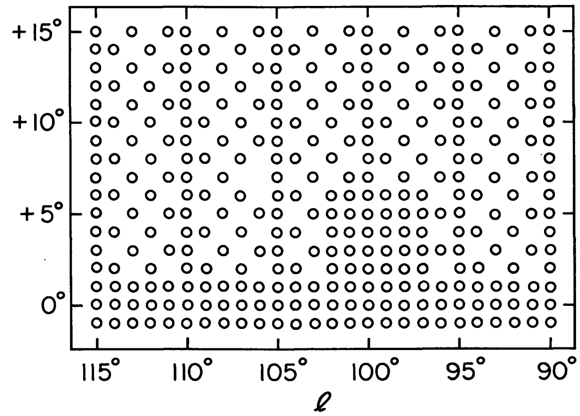

Fig. 1. Positions at which measurements were made

$-140 \mathrm{~km~s^{-1}}$ to $+60 \mathrm{~km~s^{-1}}$ with respect to the local standard of rest (LSR).

In comparing the H I distribution with that of stars, ionized gas, and dust, it is useful to display the H I column density as it appears on the sky. One would prefer to do this for intervals in distance, but since it is the line-of-sight velocity which is observed, it is more direct to take velocity intervals.

The H I column density is directly proportional to the integral of the line profile expressed as optical depth. In converting from brightness temperature, T_b, to optical depth, τ, a spin temperature of $T_s = 125$ K was adopted in the formula,

$$\tau = -\ln\left[1 - \frac{T_b}{T_s}\right]. \tag{2.1}$$

To show the appearance of the neutral hydrogen on the sky, we have constructed contour maps of optical depth in the 21-cm line as a function of ℓ and b, holding V fixed, i.e., $\tau(\ell, b|V)$ or simply $\tau(\ell, b)$ maps. The orthogonal maps in brightness temperature, $T_b(\ell, V|b)$ and $T_b(b, V|\ell)$, were used to study the characteristics of concentrations revealed by the $\tau(\ell, b)$ maps.

Figure 2 shows the $\tau(\ell, b)$ maps with τ averaged over $5 \mathrm{~km~s^{-1}}$ intervals in velocity. The velocity range of $+9$ to $-25 \mathrm{~km~s^{-1}}$ covers distances out to about 1.7 kpc at $\ell = 115°$ and out to about 4 kpc at $\ell = 90°$, according to the Schmidt (1965) rotation curve. One must keep in mind, however, that large peculiar velocities occur in the region, as indicated by the "forbidden" positive velocities seen in some of the maps.

b) Other Radio and Optical Observations

The $\tau(\ell, b)$ maps were compared with sky maps of other types of data, all brought to a common scale: the Palomar Observatory Sky Survey (POSS), spectrographic and photometric surveys of stars, atlases of dust clouds, and surveys of continuum radiation. Figure 3 summarizes the radio and optical data.

In Fig. 3(a), the highest contours of the $\tau(\ell, b)$ maps covering the range $V = -15$ to $+9 \mathrm{~km~s^{-1}}$ have been integrated to bring out the main features above the background. Regions of large column density are labeled with roman numerals, those of low column density with capital letters.

Figure 3(b) shows dust clouds and bright nebulae from Khavtassi's (1960) atlas. Three levels of shading represent the varying opacity of the dust clouds.

Figure 3(c) shows the radio continuum at 820 MHz as observed at Dwingeloo by Berkhuijsen (1972). One should bear in mind that the values of brightness temperature at the H I line frequency, 1420 MHz, are less than at 820 MHz. The reduction factor is 0.33 for thermal sources and 0.24 for the nonthermal background with an assumed spectral index of -2.6.

Figure 3(d) shows luminous stars (M_V brighter than $-1\overset{\mathrm{m}}{.}9$) and Orion-population variables. As an attempt at showing perspective, the size of symbol has been made smaller as the distance increases. The luminosity classes of the stars are also indicated in order to suggest the evolutionary state of the stellar groupings. In addition to the luminous stars, stars in reflection nebulae and T-Tauri variables and related emission-line objects are also shown.

The stellar data were taken from Blanco *et al.* (1968), Simonson (1968), and Garrison (1970). Outlines of Cep OB2 and Cep OB3 were taken from the latter two authors, respectively. Here, as elsewhere in this paper, the intrinsic B–V colors come from FitzGerald (1970). The absolute magnitudes were taken from Weaver and Ebert (1964) for luminosity classes V, IV, and III or Blaauw (1963) for classes II and I. Stars in reflection nebulae and the outlines of the R-associations were taken from Racine (1968). The emission-line variables of the Orion population were taken from Herbig and Rao (1972) and Grasdalen *et al.* (1973).

3. An Overview of the Region

We have identified five major concentrations of H I and two particularly interesting regions of low H I density in Fig. 3(a). They are numbered and lettered in order of increasing galactic longitude, but conceptually it is better to consider them in order of distance from the sun.

Let's first consider the stellar features shown in Fig. 3(d) and the dust clouds in Fig. 3(b). In distance there are three groupings. Nearest the sun are Cep R2 (400 pc), the H II region S 129 (Sharpless, 1959) (400 pc), and a few evolved stars, β, δ and ζ Cephei. Probably NGC 7023 and the associated T-Tauri variables are also at about 400 pc. The large dust cloud Kh 141 appears to lie also at 400 pc (Section 4), and probably so do the T-Tauri variables at $\ell = 90°$, $b = +2°$, since they appear to be in dust of the same complex.

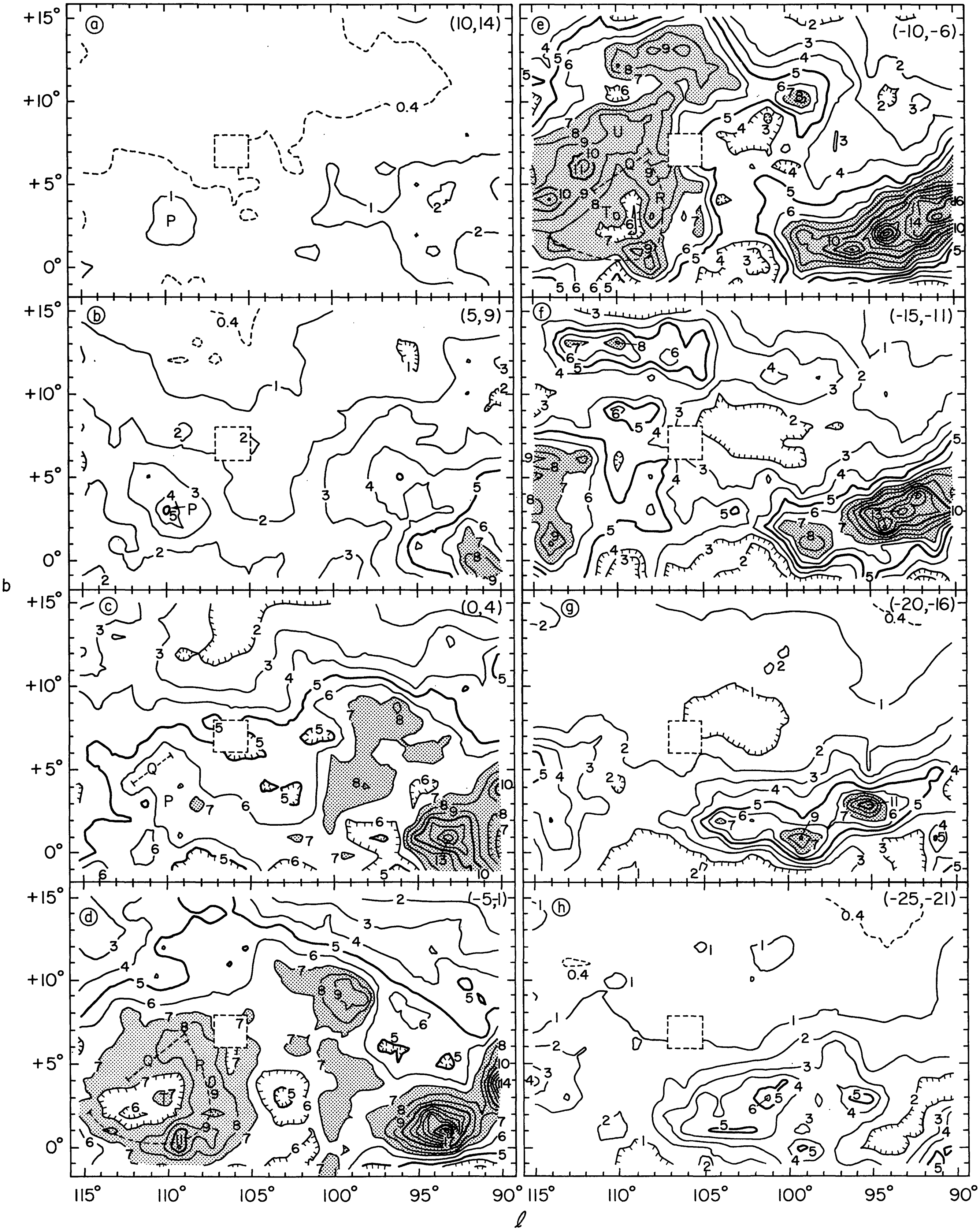

Fig. 2. Maps of optical depth in the 21-cm line, assuming $T_s = 125$ K, over 5 km s^{-1} intervals in velocity. Contours are spaced at intervals of 0.1 until 5.0, then at 0.2. Cross-marked contours surround regions of lower intensity, including also those contours intersecting one side. The maps have been left blank around a missing measurement at $\ell = 106°$, $b = +7°$

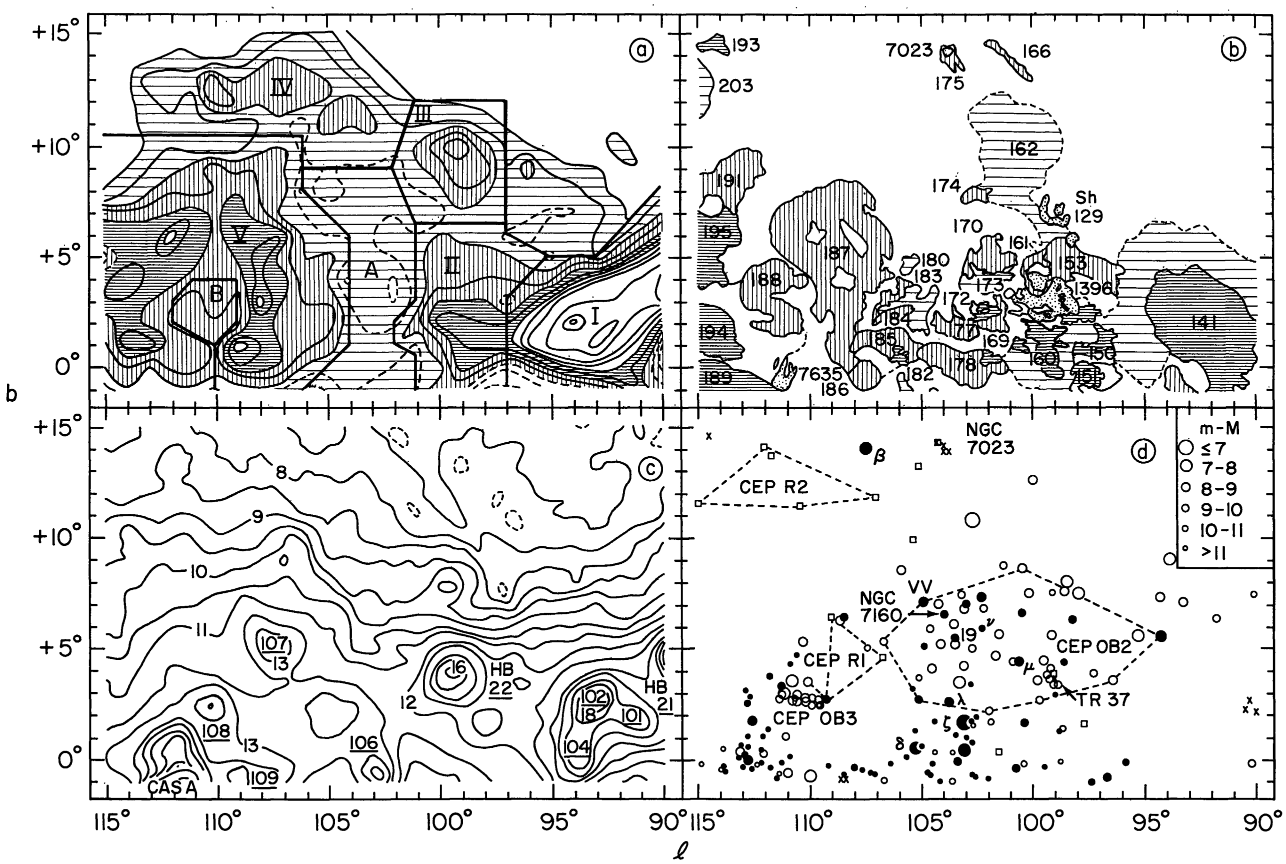

Fig. 3. (a) Contours of H I optical depth obtained by summing only the values of τ exceeding 0.5 in Fig. 2 over the velocity range $-15 \leqq V \leqq +9$ km s^{-1}. Labelled regions are discussed in the text. (b) Dust clouds and bright nebulae taken from Khavtassi's (1960) atlas. The Kh clouds (3-digit numbers) have three levels of obscuration indicated by the shading. Bright nebulae are stippled and labelled with their Sharpless (1959), NGC, or IC numbers. (c) Contours of brightness temperature at 820 MHz by Berkhuijsen (1972), who states: "The half-power beamwidth is 1°2. Absolute full beam brightness temperatures are obtained by adding 0.9 K to the contour values, which run from 4.5 step 0.5 to 11, step 1 to 18, step 2 to 26, etc." Sources have CTB numbers, underlined, except HB 22. (d) Luminous stars ($M_V < -1^m9$) are indicated by circles, with the size of the circle indicating the distance modulus. Open circles denote luminosity classes V and IV, closed circles classes III, II and I. Multiplicity of visual multiples with separately observed spectra is shown by cross marks. Orion-population variables are indicated by crosses. Stars in reflection nebulae are indicated by squares

About twice as far from the sun are the associations Cep OB 2 and Cep OB 3, at 800–830 pc. Cep OB 2 contains an O-type cluster, Trumpler 37, in an H II region, IC 1396 (the radio source HB 22). Several of the Khavtassi dust clouds in this direction are involved with the H II region, since they have bright rims. The dust clouds Kh 187 and 188 appear to surround Cep OB 3, and Cep R 1 also has the distance of 830 pc. These same clouds hide the complex thermal radio source CTB 107, but some Hα radiation, forming S 140, manages to penetrate near the edge. This whole region between 800 and 900 pc is a huge conglomerate of massive dust clouds and numerous early-type stars. It contains several centers of star formation, some active recently, others longer ago.

Finally, at 3 to 5 kpc, a third group of luminous stars appears. These are mostly evolved stars in the Perseus arm. They lie along the lower edge of Fig. 3(d), between $b = -1°$ and $+2°$.

The luminous stars and other young stellar objects, as well as the major dust clouds, fall into three groups, at 400, 830 and 4 kpc from the sun. We shall only consider here the hydrogen associated with the nearest two.

In this range of longitude and distance, radial velocities fail to yield reliable kinematic distances. In a few places, absorption against continuum sources places an upper limit on the distance. For getting distances for the neutral hydrogen, we shall be forced to rely on correlating H I features with dust clouds, in position and outline. Distances to the dust clouds are found from photometric distances to stars, either stars in reflection nebulae or stars over a range of distance that show the onset of reddening.

As we shall describe in the next sections, the H I features appear to fall into two groups—Regions I, III and IV associated with the optical features at ~400 pc, and Regions II, V, A and B associated with the optical features at ~800 pc. In the nearer region the presence of

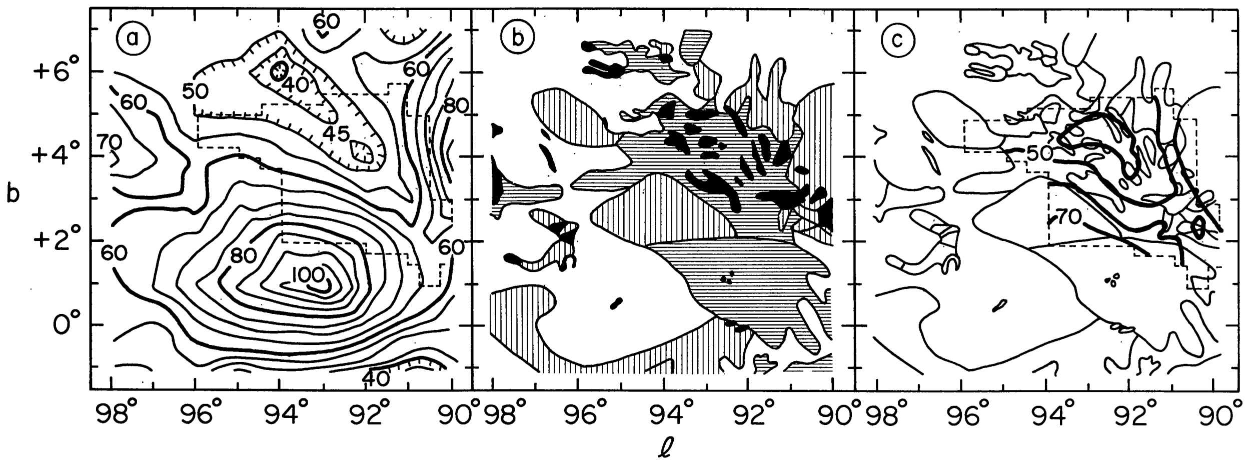

Fig. 4a—c. Self-absorption feature associated with Kh 141. (a) $T_b(\ell, b)$ contour map for $V = -3\,\mathrm{km\,s^{-1}}$, with the region where profiles show self-absorption dips outlined by a dashed line. (b, c) Dark clouds as shown in Lynds's (1962) atlas, with the contours of T_a at the bottom of the self-absorption dip superimposed (from Weaver and Williams, 1973)

Orion-population variables suggests we may be witnessing star formation in its earliest stages here. In the farther region star formation has gone on for a long time, and we now see several subgroups with a range of ages. So in evolutionary state as well as in age, the two regions are distinct. The local kinematics and structure of the neutral hydrogen are of interest in connection with these stages in the development of clusters and associations of young stars. We discuss the details of each region seperately in the following sections.

4. Region I, Cool Hydrogen in the "Northern Coalsack", Kh 141

The high optical depth found in Region I is due primarily to the effects of differential rotation at this longitude. These effects give $V \approx 0$ for all the H I out to several kiloparsecs from the sun. Adding to the high optical depth in Region I is a feature of the galactic spiral structure that Westerhout (1957) called an intermediate arm between the Orion and Perseus arms.

The main importance of the high T_b in Region I for the present purposes is it serves as a hot background. Against this background cooler H I associated with Kh 141 can be seen as a self-absorption feature. The self-absorption occurs as a sharp dip in the H I line profiles at velocities between -2 and $-3\,\mathrm{km\,s^{-1}}$.

Fig. 4 as it appears in the 21-cm line and in Lynds's (1962) atlas of dark nebulae. The effects of the background on the appearance of Fig. 4 can be judged by looking at Fig. 2. Figure 2(d) contains the self-absorption feature, while Fig. 2(c) and 2(e) cover velocity ranges on either side. Absorption against the continuum background from CTB 102 and 101 [Fig. 3(c)] may contribute slightly to the dip in the profiles along the lower-latitude edge, but the continuum brightness temperature only amounts to about 6 K at most.

We can get a better idea of where the cold hydrogen is by using Weaver and Williams' (1973) profiles, which were observed on a finer grid than ours. In Fig. 4(b) the contours of their antenna temperature, T_a, at the center of the self-absorption dip are superimposed on Lynds's map. [Comparison of the profiles in the region suggests the temperature scales are nearly the same in the sense $T_b\,(\text{Dwingeloo}) / T_a\,(\text{Berkeley}) \approx 1.05$. Williams (1973), however, finds $T_b/T_a = 1.18$ for extended sources in the Berkeley survey.]

The strongest self-absorption is found along the line of the darkest clouds, but the 21-cm line contours do not have the same shape as the dark clouds.

Knapp (1972) was able to obtain the optical depth in one of two positions she observed in the region, using the NRAO 140-foot telescope with $0.3\,\mathrm{km\,s^{-1}}$ resolution. She assumed a gaussian function for the optical depth, namely

$$\tau = \tau_0 \exp\left[-\frac{(V - V_0)^2}{2\sigma^2}\right], \tag{4.1}$$

with T_b given by the expression,

$$T_b = T_s(1 - e^{-\tau}) + T_g e^{-\tau}, \tag{4.2}$$

where T_g is the background brightness temperature. At $\ell = 92.^\circ4$, $b = +2.^\circ4$, she found $T_s = 29\,\mathrm{K}$, $\tau_0 = 1.0$, $\sigma = 0.86\,\mathrm{km\,s^{-1}}$ and $V_0 = -2.82\,\mathrm{km\,s^{-1}}$. The H I column density is given by

$$N_\mathrm{H}[\mathrm{cm^{-2}}] = 1.823 \times 10^{18} \int T_s[\mathrm{K}]\tau dV[\mathrm{km\,s^{-1}}], \tag{4.3}$$

or, substituting expression (4.1),

$$N_\mathrm{H} = 1.823 \times 10^{18} (2\pi)^{1/2} T_s \sigma \tau_0 . \tag{4.4}$$

Knapp found $N_\mathrm{H} = 1.5 \times 10^{20}\,\mathrm{cm^{-2}}$.

From our own observations we may roughly estimate T_s and τ_0 in the cool H I throughout the cloud by assuming: (i) there is no H I between the sun and the cloud at the velocity of the cloud; (ii) T_s and τ_0 are uniform in the cool cloud; (iii) the background brightness temperature has contours of the same shape as the τ contours of Fig. 2(e), at a velocity just off the self-absorption dip. The T_b values of the background are given by Fig. 4(a) at positions just outside the dashed region, i.e., we use the τ contours at $V=-10$ to -6 km s^{-1} to interpolate T_g.

With these assumptions, the self-absorption positions give mean values of $T_s \sim 39 \pm 27$ K and $\tau_0 \sim 0.8 \pm 0.4$. Clearly our assumptions are indeed crude. However, in Weaver and Williams's (1973) observations, the minimum value of T_a ($\approx$ our T_b) in the self-absorption dip is 38 K, found at $\ell = 92.°0$, $b=+3.°75$, $V=-2$ km s^{-1}. This is an upper limit on T_s at this point. Our value of T_s may be fairly representative. The value for τ_0 is only moderately high. Therefore the contours within the dashed region of Fig. 4(a) are still significantly affected by the background and are not simply contours of cool hydrogen.

The distance to Kh 141 can be roughly estimated from the data of Blanco *et al.* (1968) and Simonson (1968). In the direction of Kh 141 the most distant unreddened stars are HD 200943 and HD 201431, both A 0, at distance moduli $\varrho = 7.^m1$ and $6.^m9$, respectively. [This tends to justify assumption (i) above.] The nearest reddened stars are HD 200857, B3 III, $\varrho = 8.^m9$ and HD 198512, B1 V, $\varrho = 9.^m1$. For the distance to Kh 141 we adopt the mean in distance modulus, $\varrho = 8^m \pm 1^m$, or $R = 400^{+230}_{-150}$ pc.

If we take $T_s \approx 40$ K and $\tau \approx 0.8$ with $\sigma \approx 1$ km s^{-1}, then the mean $\langle N_H \rangle \approx 0.8 \times 10^{20}$ cm^{-2}. The mass of H I is given by

$$\mathcal{M}[\mathcal{M}_\odot] = 4.44 \iint T_s[\mathrm{K}]\tau(R[\mathrm{kpc}])^2 dV[\mathrm{km\,s^{-1}}]d\Omega[\mathrm{deg}^2]\,. \quad (4.5)$$

Over the 15.5 deg^2 area of the self-absorption feature, the mass of cold H I is about $\mathcal{M} \approx 1 \times 10^5$ $\mathcal{M}_\odot$ at $R=400$ pc. If the thickness of the cloud corresponds to the mean angular dimension of about 4°, then the mean density of cool neutral hydrogen is about $n_H \approx 1$ cm^{-3}. Kh 141 therefore appears to be a complex of dust and gas consisting of a diffuse envelope with an elongated inner core of small, irregular, dense dust clouds. It contains cool neutral hydrogen that appears to be only moderately opaque on a scale of 0.°6. The presence of the T-Tauri-type stars may indicate recent star formation in the dark clouds. The complex of continuum sources behind the dark cloud also indicates the presence of young stars in H II regions in this direction, but as their distances are unknown, their relation to Kh 141 cannot be assessed.

5. Region III, the Concentration at $\ell = 99°$, $b = +10°$.

The H I in Region III appears to be associated with the dust cloud Kh 162 by virtue of the similarity in size and position. Photoelectric data from Simonson (1968) and Blanco *et al.* (1968) show two unreddened stars in the direction of Kh 162 at $\varrho = 6.^m4$ ($R=190$ pc), namely, HD 201888, B 8, and HD 203467, B 3 Ve. One unreddened star, HD 203550 A, A 0, lies just off the edge, at $\varrho = 7.^m5$ ($R=320$ pc). Three reddened stars with $E_{B-V} = 0.4$ to 0.7 are found in the range $\varrho = 7.^m4$ to $8.^m4$ ($R=380$ to 480 pc), namely, HD 202214, B0V, HD 239618, B 2 Ve, and HD 203374, B 0 IV pe. Two stars at roughly twice the distance have about the same reddening, HD 239595, B2 v, at $\varrho = 9.^m6$ ($R=830$ pc) with $E_{B-V} = 0.4$ and BD+61°2127, B1.5V, at $\varrho = 9.^m7$ ($R=860$ pc) with $E_{B-V}=0.8$. The distance of Kh 162 is therefore probably about $R \approx 400$ pc.

The H II region S 129 lies on the lower side of the dust cloud and the H I concentration. Although large in angular size, S 129 is only a weak thermal source, as is evident from Fig. 3(c). Its exciting star is HD 202214. The radial velocities of the H I concentration and HD 202214 are the same, $V=-3$ km s^{-1}.

The general background at the latitude of the concentration has an optical depth of $\tau \approx 0.5$. Knapp (1972) found no evidence for self-absorption at $\ell = 99°$, $b=+10°$. We estimate the mass in the concentration by integrating within the contours $\tau = 0.6$ to 0.9. The result is $\mathcal{M} = 5.5 \times 10^3 R^2[\mathrm{kpc}^2]\mathcal{M}_\odot$. If $R=400$ pc, then $\mathcal{M} = 900\,\mathcal{M}_\odot$.

6. Region IV, the Concentration around Cep R 2

Although Khavtassi's atlas gives no indication of dust clouds in Region IV, obscuration does appear in large-scale photographs in the direction of this H I concentration. The region also forms part of the "Cepheus flare," an extension of the zone of avoidance found in galaxy counts (cf. Steinlin, 1962). The H I concentration is also associated with a number of small, dense dust clouds and Orion-population variables. Its angular size and position corresponds closely to Cep R 2 (Racine, 1968). Racine found $R = 400 \pm 80$ pc from six stars in reflection nebulae. If this is also the distance to the H I concentration, its height above the galatic plane is 80 pc, which is not unreasonable.

The mass in Region IV is estimated in a slightly different way than in Region III since the profiles are more regular and can be represented in the form of single gaussians. We measure τ and σ at each position, assuming $T_s = 125$ K. Equation (4.4) then gives N_H, and the mass is found from the expression

$$\mathcal{M}[\mathcal{M}_\odot] = 2.44 \times 10^{-18} \int N_H[\mathrm{cm}^{-2}]R^2[\mathrm{kpc}^2]d\Omega[\mathrm{deg}^2]\,. \quad (6.1)$$

Over the 32 deg^2 of the concentration we find $\langle V_0 \rangle = -8.8$ km s^{-1}, $\langle \sigma \rangle = 3.9$ km s^{-1} and $\langle \tau_0 \rangle = 0.92$, giving $\langle N_H \rangle = 2.0 \times 10^{21}$ cm^{-2}. The total H I mass is then $\mathcal{M} = 16.0 \times 10^4 R^2[\mathrm{kpc}^2]\mathcal{M}_\odot$. Outside the concentra-

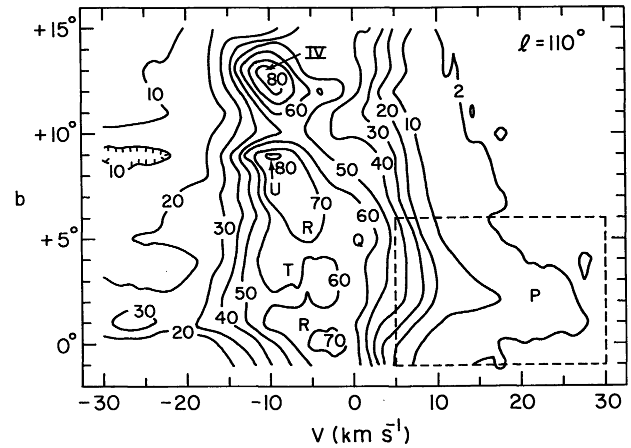

Fig. 5. $T_b(b, V)$ contours in units of K for $\ell = 110°$. Features belonging to the shell around Cep OB3 are labelled, as is Region IV

tion at the same latitude we find $\langle \tau_0 \rangle = 0.65$. Thus the mass of foreground and background H I is $\mathcal{M} = 12.0 \times 10^4 R^2 [\mathrm{kpc}^2] \mathcal{M}_\odot$, giving $\mathcal{M} = 4.3 \times 10^4 R^2 [\mathrm{kpc}^2] \mathcal{M}_\odot$ for the concentration. Taking $R = 400$ pc, then $\mathcal{M} = 7 \times 10^3 \mathcal{M}_\odot$. This result is uncertain owing to the crude assumptions and large correction.

Of particular interest is the association of this concentration with recent star formation. Several of the stars in the reflection nebulae are T-Tauri or FU-Orionis stars, generally considered to be pre-main-sequence objects. Strom *et al.* (1972) have found several stars with large infrared excesses in a small region around the bright reflection nebula NGC 7023; they interpret these also as pre-main-sequence stars. At the higher-longitude side, this concentration joins the region studied by Heiles (1976). We discuss this further in Section 9(b).

7. Cep O B 3 and Its Surrounding Ring of Clouds

In Fig. 3 Cep OB3 lies in a low-intensity region, Region B, surrounded by a ring of H I in Region V. It seems natural to consider whether this gas forms an expanding shell around the association.

The H I structure around several associations has been interpreted as expanding shells. For example, Menon (1958) found such a shell around Ori OB1, as did Girstein and Rohlfs (1964) around Mon OB1 and Howard (1958) around Lac OB1. Recently, Sancisi (1974) found evidence for a shell in the region of Per OB2, but suggested the stars have moved to the outside of the shell. In many cases only a partial shell is found, and frequently it is hard to be sure of the association of the H I features and the stellar ones.

Around Cep OB3 we have a favorable set of circumstances for investigating the presence of a shell. At this galactic longitude, galactic differential rotation allows only negative velocities. Any gas at the distance of the association with appreciable positive velocity exceeding ~ 10 km s^{-1} will be separated from the gas in the general field. The association also contains the thermal radio source CTB 108 in the H II region S 155. This radio source may serve as a continuum background for H I absorption and allow us to distinguish gas in front of the association from that behind it.

a) Summary of Optical Data

Figure 3(d) shows that Cep OB3 is much more compact than Cep OB2. It contains more than 20 stars earlier than B1 in an area of only 9 deg^2 despite its distance of only 800 pc (Garrison, 1970).

The surrounding ring-shaped complex of dust, Kh 187 and 188, has a prominent appearance in wide-angle photographs. Garrison (1970) remarks, "similar rings have been noted by Morgan and the author on a number of plates of distant H II regions."

Cep OB3 contains two subgroups, Cep OB3a of age 8×10^6 yr, and Cep OB3b of age 4×10^6 yr (Blaauw, 1964). The younger subgroup contains S 155. Garrison (1970) notes, "curiously, the O-type stars do not seem to be connected with much nebulosity," and he remarks that the exciting star of the H II region has probably not yet been found.

The radial velocities of the stars in Cep OB3 range from 0 to -30 km s^{-1} (Garmany, 1973), making the standard radio-line correction to the LSR (Kerr, 1965). Their mean is -11 km s^{-1}, but Garmany finds the mean radial velocity of the younger subgroup to be 4 km s^{-1} more negative than that of the older.

b) Summary of H I Data

The various features of the H I structure in the region of Cep OB3 have been labeled alphabetically, *P* through *U*, in Fig. 2. The velocity structure can also be followed in the $T_b(b, V)$ map at $\ell = 100°$ shown in Fig. 5. These features include: P, a positive-velocity concentration in the direction of Cep OB3; *Q*, a ridge just above Cep OB3; *R*, an arc-shaped feature that joins with feature *Q* to encircle Cep OB3; *T*, a concentration in the direction of the H II region CTB 108; and *U*, a large ridge of emission. The appearance of the maps is strongly influenced in several small regions by absorption against continuum sources.

The emission features *Q* and *R* are associated with the dark clouds Kh 187 and 188. We shall interpret features *P*, *Q* and *R* as an expanding shell around Cep OB3. Feature *T* is associated with dark clouds near the center of the association. Feature *U* seems to have less connection with Cep OB3. We shall now consider this H I structure in more detail.

c) The Positive-Velocity Feature P

Feature *P* appears right in the direction of Cep OB3 at $\ell = 110°$, $b = +3°$, in Figs. 2(a) and 2(b). We have

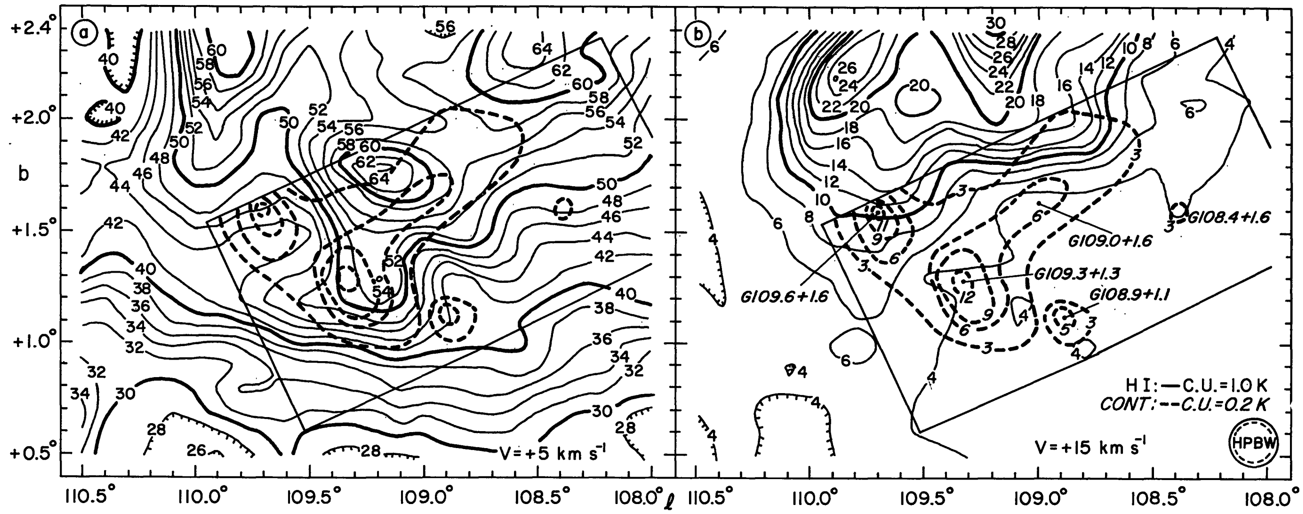

Fig. 6a and b. Comparison of 21-cm continuum (dashed contours, Felli and Churchwell, 1972) and H I line (solid contours, Westerhout, 1973) emission in the region of Feature *P*. (a) Lower-velocity component at $+5\ \mathrm{km\ s^{-1}}$. (b) Higher-velocity component at $+15\ \mathrm{km\ s^{-1}}$. Note difference in contour units (c.u.) between continuum and line. For clarity, only the contours at 0.6 K intervals and at maxima are shown from Felli and Churchwell

outlined it also in Fig. 5. These positive velocities extending to greater than $+25\ \mathrm{km\ s^{-1}}$ are "forbidden" in pure differential rotation between $\ell=90°$ and 180°. With only one exception, no such excursion into forbidden positive velocities may be found in this whole quadrant of galactic longitude in the maps of Weaver and Williams (1974a) or Burton and Verschuur (1973). [The lone exception is a somewhat similar feature between $\ell=87°$ and 92°, $b=+5°$ to $+7°$, which is visible in part in Fig. 2(a). This is also the position of the supernova remnant HB 21, and it may not be surprising to find peculiar H I motions in such a location.]

Feature *P* contains two components at different velocities. As shown in Fig. 2(b) and 5, the stronger component reaches a maximum at $V=+5\ \mathrm{km\ s^{-1}}$ near $\ell=110°$, $b=+3°$. At medium resolution it appears as a shoulder on the line profiles, but Westerhout's (1973) 300-ft observations show a separate peak from $\ell=108\overset{\circ}{.}7$ to $109\overset{\circ}{.}5$ between $b=+2\overset{\circ}{.}0$ and his survey limit at $b=+2\overset{\circ}{.}4$. Figure 6(a) shows more detail of the structure at $V=+5\ \mathrm{km\ s^{-1}}$. The peak T_b is about 65 K.

A weaker component extends to nearly $V=+30\ \mathrm{km\ s^{-1}}$. It reaches a peak near $V=+15\ \mathrm{km\ s^{-1}}$. Figure 6(b) shows the angular structure. It has at least two separate maxima, one extending above Westerhout's survey limits at $\ell=109\overset{\circ}{.}1$, $b\geqq+2\overset{\circ}{.}4$, $T_b\geqq31$ K, the other lying at $\ell=109\overset{\circ}{.}9$, $b=+2\overset{\circ}{.}2$, $T_b=26$ K.

In order to sort out the distance relation between Cep OB3 and the gas in Feature *P*, we have examined the H I observations for evidence of absorption against CTB 108. None is apparent, but we have only low angular resolution in the continuum and medium resolution in H I.

In Fig. 6 we show the available high-resolution continuum and H I line observations in the region of Feature *P*. We have labeled the separate sources with their galactic coordinates. G 109.0+1.6 agrees with the H II region S 154 in shape and position, but the stronger sources lie behind opaque dust. S 154 probably belongs to the Cep OB3 complex. It is a diffuse H II region, visible on both red and blue plates. Yet it is apparently involved in the dense dust that extends over CTB 108. Its exciting stars are unidentified.

In frequency-switched observations, the effect of a continuum source of brightness temperature T_c lying beyond a uniform H I layer of optical depth τ is to decrease the H I T_b in the direction of the source by an amount

$$\Delta T_b = T_c(1-e^{-\tau})\,. \tag{7.1}$$

For opaque H I, the maximum ΔT_b would be about 2 K for these sources.

The lower-velocity component in Fig. 6(a) shows no evidence of absorption. The continuum peaks lie on the shoulders of the line peaks, often on local ridges of line emission. The higher-velocity component in Fig. 6(b) apparently fails to coincide with the continuum sources, except for G 109.6+1.6. Again, there is no evidence of absorption against this source. (There may be absorption against G 109.3+1.3, but if so, it may be occurring in foreground H I. The minimum is of the same order as the fluctuations all over the map well off Feature *P*.)

The available observations show no evidence of absorption against CTB 108 or S 154; we are led to conclude the gas lies on the far side of the H II regions and is moving away both from them and from us. In view of the coincidence in direction with Cep OB3, and considering that the association is a source of thermal energy which could conceivably result in large motions of surrounding gas, it seems natural to relate Feature *P* to the association.

As an upper limit to the mass in Feature P we have taken all the H I emission at velocities above 5 kms^{-1}. The correction for the general background is small at these velocities: $\tau_g = 0.2$ for $V = +5$ to $+9\,\mathrm{km\,s^{-1}}$ and $\tau_g \approx 0.0$ above $V = +10\,\mathrm{km\,s^{-1}}$. We find $\mathcal{M} = 8 \times 10^3 \mathcal{M}_\odot$ at $R = 800$ pc. The mean velocity of this hydrogen is $\langle V \rangle = +49\,\mathrm{km\,s^{-1}}$. As a lower limit on the mass, we may take the H I at velocities above $+15\,\mathrm{km\,s^{-1}}$ (shown in Fig. 5 but not in Fig. 2). The total mass is then $\mathcal{M} = 1 \times 10^3 \mathcal{M}_\odot$ at $R = 800$ pc, and $\langle V \rangle = +16\,\mathrm{km\,s^{-1}}$. We shall discuss the kinetic energy of Feature P after examining Features Q and R.

d) Features Q *and* R, *the Ring around* Cep OB 3

Moving toward lower velocities, a sort of ridge appears toward the upper left of Cep OB 3 in Fig. 2(c) and 2(d). We have labeled it Q. It reaches a peak T_b of about 65 K at $V = 0\,\mathrm{km\,s^{-1}}$ as a shoulder on the H I line profile (Fig. 5). It corresponds in position to the upper portion of Kh 188 and to part of Kh 187 in Fig. 3(c). At greater negative velocities it tends to blend with Feature U, as can be seen in Fig. 2(e) and Fig. 5.

We have estimated the mass in Feature Q from $\tau(\ell, b)$ maps constructed over $2\,\mathrm{km\,s^{-1}}$ intervals in velocity. Because of blending with Feature U the background correction is harder to judge; it increases almost linearly from $\tau_g = 0.2$ at $V = +6$ to $+7\,\mathrm{km\,s^{-1}}$ to $\tau_g = 0.6$ at $V = -4$ to $-3\,\mathrm{km\,s^{-1}}$. The feature covers 15 deg^2, and we have followed it over the velocity range $V = -4$ to $+7\,\mathrm{km\,s^{-1}}$. Its mass is $\mathcal{M} = 9 \times 10^3 \mathcal{M}_\odot$ at $R = 800$ pc. Its mean velocity is $\langle V \rangle = +1\,\mathrm{km\,s^{-1}}$.

Continuing into negative velocities, an arc-shaped H I concentration, labelled R, appears in Fig. 2(d), surrounding Cep OB 3 on the right and bottom and joining with Feature Q at the top to encircle the association. Its peak T_b is 87 K at $\ell = 109°$, $b - 0°$, $V = -4\,\mathrm{km\,s^{-1}}$. Feature R corresponds to the main portion of Kh 187 plus Kh 194. Feature R covers an area of 32 deg^2 through the velocity range $V = -12$ to $+3\,\mathrm{km\,s^{-1}}$. We estimate the background optical depth on the $2\,\mathrm{km\,s^{-1}}$ maps as $\tau_g = 0.5$ over this range, except between $V = -2$ to $+1\,\mathrm{km\,s^{-1}}$, where $\tau_g = 0.6$. The mass of Feature R above this background is $\mathcal{M} = 3 \times 10^4 \mathcal{M}_\odot$, and its mean velocity is $\langle V \rangle = -5\,\mathrm{km\,s^{-1}}$.

e) The Connection of Other H I *Features with an Expanding Shell*

At larger negative velocities shown in Figs. 2(e) and 2(f) it becomes more difficult to judge which H I features should be associated with Cep OB 3. More and more H I in the general galactic field appears in the maps. However, a local maximum in the H I emission persists in the direction of Cep OB 3 throughout the velocities shown in Figs. 2(e)–2(g). There is therefore no contradiction to the expanding shell interpretation.

A small concentration, labeled T, appears in the direction of Cep OB 3 in Fig. 2(d) and 2(e). Feature T covers about 3 deg^2 at latitudes along the upper edge of Cep OB 3, and its velocity is very close to the mean stellar velocity. It reaches a peak T_b of 66 to 68 K at $V = -8\,\mathrm{km\,s^{-1}}$ along the line $\ell = 110\overset{\circ}{.}0$ to $111\overset{\circ}{.}5$ at $b = +3\overset{\circ}{.}5$ in Weaver and Williams' (1973) profiles.

A slight dip which may be due to absorption occurs in the profile of Feature T in the direction of CTB 108. As may be seen in Fig. 3(b), CTB 108 rises 4 K above the background at 820 MHz. Assuming it is unresolved both by Berkhuijsen and by Weaver and Williams, then T_c should be ~ 7 K above the background for CTB 108 at 1420 MHz. The observed ΔT_b is $\lesssim 2$ K at $\ell = 110\overset{\circ}{.}5$, $b = +2\overset{\circ}{.}75$, $V = -8\,\mathrm{km\,s^{-1}}$, which would not disagree with Eq. (7.1). It indicates Feature T lies in front of CTB 108.

In addition to Feature T, a smaller concentration covers a wider velocity range from $V = -3$ to $-12\,\mathrm{km\,s^{-1}}$ in an area of 0.5 deg^2 surrounding CTB 108. On a smaller scale this central region resembles the entire complex around Cep OB 3. The mass is about $\mathcal{M} = 500 \mathcal{M}_\odot$ at $R = 800$ pc.

An estimate of the H I mass in front of Cep OB 3 may be made from the relation of color excess and H I column density. Kerr and Knapp (1974) find $N_H/E_{B-V} \simeq 5 \times 10^{21}$ atom cm^{-2} mag^{-1}. Garrison (1970) finds the foreground color excess to be $E_{B-V} = 0.5$ mag. Over the area of the association he finds up to an additional 0.5 mag, with an average of about 0.25 mag. Let us suppose $E_{B-V} = 0.25$ mag from dust lying just in front of the association. Then over a 3 deg^2 area $\mathcal{M} = 6 \times 10^3 \mathcal{M}_\odot$ at $R = 800$ pc, which would be comparable to Feature P.

The long ridge of H I emission labeled U in Fig. 2(e) we feel should not be included in the Cep OB 3 complex. From its position in the sky it could as well be associated with Cep OB 4, at $\ell = 118\overset{\circ}{.}0$, $b = +5\overset{\circ}{.}2$. Also, Feature U seems to occupy a clear region, coinciding with only a portion of one dust cloud, Kh 194, at $\ell = 114°$, $b = +4°$. This is unlike Features Q and R, which correspond to dense dust clouds involved in the association. From its velocity of $V = -9\,\mathrm{km\,s^{-1}}$ (Fig. 5), Feature U could also be associated with the hydrogen in Region IV.

f) Continuum Sources and H I *in the* Cep OB 3 *Region*

In the region of Cep OB 3, local minima in the line profiles occur mostly near $V = -6\,\mathrm{km\,s^{-1}}$. For comparison with continuum sources and dark clouds, Fig. 7 shows (a) contours of the H I at $V = -6\,\mathrm{km\,s^{-1}}$, (b) continuum sources from Felli and Churchwell (1972) at 1414 MHz or Berkhuijsen (1972) at 820 MHz, and (c) dark clouds from Lynds's (1962) atlas together with H II regions from Sharpless's (1959) catalogue. The H I contours were made from Weaver and Williams' (1973) profiles above $b = +2\overset{\circ}{.}5$ and from Westerhout's (1973)

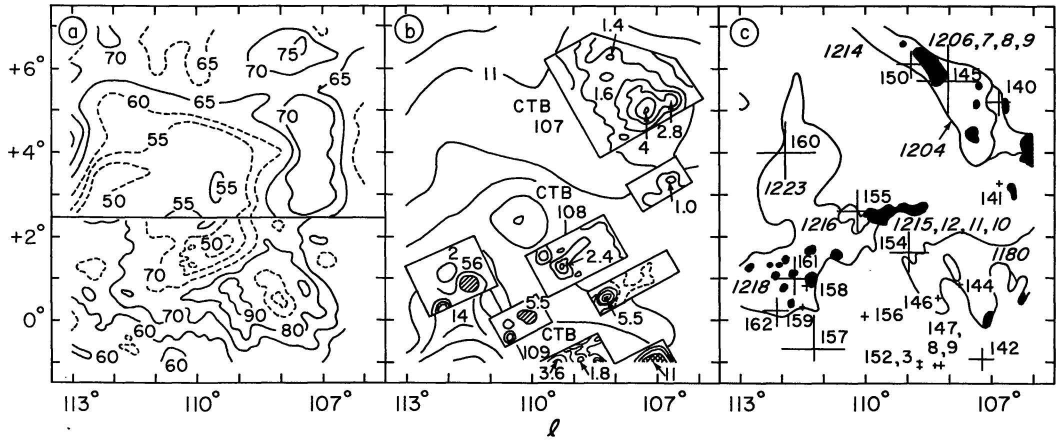

Fig. 7. (a) H I contours in units of K for $V=-6\,\mathrm{km\,s^{-1}}$ constructed from Weaver and Williams' T_a (1973) profiles (top) and from Westerhout's (1973) T_b data (bottom). (b) Contours of continuum brightness temperature from Felli and Churchwell's (1972) survey at 1414 MHz (inserts) superimposed on Berkhuijsen's (1972) 820-MHz survey. Contour intervals for the inserts are mostly 1.6 K, with the lowest at 0.2 K. (c) Dark clouds from Lynds's (1962) catalogue (four-digit numbers) with the positions and largest diameters of Sharpless's (1959) H II regions marked (3-digit numbers)

survey below $b=+2.^\circ4$ (we are indebted to Mr. K.-H. Fogg for the latter map). The temperature scales have the ratio T_a(Berkeley)/T_b(Maryland-Green Bank) = 0.95 (Harten *et al.*, 1975).

The CTB 107 complex, including S 140, 145 and 150, is involved in a number of Lynds dark clouds making up Kh 187. We find a suggestion of absorption at $V=-6\,\mathrm{km\,s^{-1}}$, but only as a steepening of the shoulder of the profile. The effect is expected to be small from Eq. (7.1) since the maximum T_c is 4 K. We detect no effect of S 141.

S 106, a faint, diffuse H II region, appears to coincide with a bulge in the 820-MHz contours. We find a rather distinct dip in this region around $\ell=112°$, $b=3.^\circ5$, in the Weaver and Williams profiles, but it is more likely to be self-absorption connected with Lynds 1223 (in a small area not included in Kh 188!). In this case, the upper limit on T_s is about 50 K.

S 144 coincides with a minimum in the H I contours that seems out of proportion to its T_c of 5.5 K. This minimum is caused not by a dip in the profile tops but by a decrease in the heights of the peaks; it is a slight gap in the H I. In addition, right at the position of S 144 there is a steepening of the profile shoulder, which would not be inconsistent with $\Delta T_b < 5$ K of absorption.

The sources that make up CTB 109 appear all to lie in the Perseus arm, but the absorption effects are not pronounced. S 156 even seems to coincide with a local maximum in the H I. Its T_c is only 5.5 K, however. What is really surprising is S 158, whose T_c is 56 K, but where ΔT_b is at most 5 K. S 158 is very small and not heavily obscured, so probably there just happens to be no opaque, cool H I in its exact direction. S 162, with $T_c=14$ K, gives almost the same effect, $\Delta T_b \lesssim 5$ K.

The correlation of the dip in the line profile with dark clouds is almost anti-correlation. In other words, the dark clouds are regions of enhanced H I emission even though this velocity of $-6\,\mathrm{km\,s^{-1}}$ in Fig. 7(a) is not the velocity of the peak. Two possible exceptions in the upper part of Fig. 7 are L 1223, as already discussed, and L 1204 in the region of CTB 107. The latter does not show a dip in the line profile, however.

The lowest H I minimum in all of Fig. 7(a) occurs at $\ell=109.^\circ3$, $b=+1.^\circ8$, between S 154 and S 155. Although this region is not included as a dust cloud in either Khavtassi's or Lynds's atlas, it probably should be, because the obscuration is about the same as in the surrounding larger clouds, e.g., L 1218.

We may use these results to estimate what additional early-type stars may exist in the region of Cep OB3. The most important sources are the CTB 107 complex and S 154. S 160 is also of interest, but we lack detailed radio data, and S 141 is of minor importance.

To estimate the stellar content of these H II regions from the radio continuum flux, we use the calibration of ionizing flux from early-type stars given by Churchwell and Walmsley (1973). In particular, the ionization parameter for a zero-age main-sequence O 9 star is $U=41\,\mathrm{pc\,cm^{-2}}$.

Since the CTB 107 and S 154 regions are complex, Felli and Churchwell (1973) refrained from stating the flux densities. From their figures we estimate the total flux densities at 1414 MHz as $S=100$ Jy for CTB 107 and $S=30$ Jy for S 154. The ionization parameters are $U=50\,\mathrm{pc\,cm^{-2}}$ and $34\,\mathrm{pc\,cm^{-2}}$, respectively, assuming $R=800$ pc and an electron temperature of 6000 K. Consequently, ten or fewer B0–O9 stars would suffice in each case.

g) Discussion of Expanding Shell

In summary, the structure of the gas around Cep OB3 seems to be an expanding shell. It can be visualized from Fig. 2. In this range of longitude, differential rotation would ordinarily sort things in distance from the sun in the sense the farther the material the more negative the velocity. That has to be reversed when dealing with peculiar motions of the type found here. Figure 2(a) shows the material farthest from the sun, not closest. Then as we progress through Figs. 2(b), 2(c), 2(d) and 2(e), we are seeing slices of gas closer to the sun. It's like slicing a hard-boiled egg with the yolk removed. We have tried to indicate this in Fig. 8. Part (a) shows how the slices are cut in Fig. 2, and Part (b) shows an exploded view of how the features might be arranged. In this crude model, Features *P*, *Q* and *R* are expanding with about the same velocity of $10\,\mathrm{km\,s^{-1}}$. We see the full expansion velocity for Feature *P*, and about half of it for Feature *Q*. Feature *R* gives the dimensions of the shell, about 3° or 40 pc. At a constant $10\,\mathrm{km\,s^{-1}}$, the expansion age is 4×10^6 yr, almost the same as the age of the stellar association.

While the far side and the edge of the shell are quite evident, it is hard to tell if any expanding material lies on the near side. This should appear in Fig. 2(f) and 2(g). While there is some degree of concentration there, it could equally well be explained as distant H I in the intermediate arm. The near side of the shell should absorb CTB 108, but the expected effect is very small and we find little evidence for it.

We may estimate the kinetic energy involved in the expansion by taking the masses computed for the features and the apparent expansion velocity of $\sim 10\,\mathrm{km\,s^{-1}}$. The mass of Feature *P* is $8000\mathcal{M}_\odot$, Feature *Q* $9000\mathcal{M}_\odot$, Feature *R* $30000\mathcal{M}_\odot$ and the nearside gas $\sim 6000\mathcal{M}_\odot$, totaling $5.3\times10^4\mathcal{M}_\odot$. If it were all expanding at $10\,\mathrm{km\,s^{-1}}$, the total kinetic energy would be 5.3×10^{49} erg.

The minimum kinetic energy can be estimated from Feature *P* alone. There is no mistaking its peculiar velocity, and the lack of continuum absorption features puts it on the far side of the association. Its mean velocity is $\langle V\rangle = +9\,\mathrm{km\,s^{-1}}$. If we refer this to the velocity of Feature *R*, for which $\langle V\rangle = -5\,\mathrm{km\,s^{-1}}$, the kinetic energy of Feature *P* is 1.2×10^{49} erg.

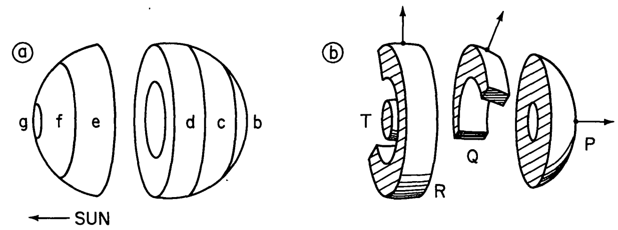

Fig. 8. (a) Schematic diagram of the shell around Cep OB3 as it appears in the sections of Fig. 2. (b) Schematic diagram of the shell around Cep OB3, showing the concentrations discussed in the text

8. H I Features in Cep OB 2

a) Region II, *near* IC *1396*

IC 1396 is a large H II region of low surface brightness excited by the stars of the early-type cluster Trumpler 37, whose distance is about 830 pc (Simonson, 1968). From Figs. 2 and 3, a general H I concentration is apparent at the position of the H II region in the velocity range of the cluster stars, $V = 0$ to $-10\,\mathrm{km\,s^{-1}}$. However, because of the effects of differential rotation at this longitude, about 80% of N_H may be due to foreground and background H I within 1.5 kpc of the sun.

This region has been the subject of a more detailed survey summarized by Simonson (1974). The detailed survey revealed several smaller H I concentrations that correspond in shape and position with the bright-rimmed dark clouds involved with the H II region. The smaller concentrations contain about $2\times10^4\mathcal{M}_\odot$ of neutral hydrogen. This may be compared with the mass of the ionized hydrogen, $7\times10^3\,\mathcal{M}_\odot$ (Pottasch, 1965), and the mass of young stars earlier than B3, $10^3\,\mathcal{M}_\odot$ (Simonson, 1968).

The higher-longitude edge of the concentration is quite abrupt. We shall discuss the significance of this later in connection with Region A.

We also note that expansion of the gas seems to be taking place in IC 1396, away from the central cluster, Tr 37. This is inferred from the current picture of the evolution of H II regions (Pottasch, 1965). IC 1396 is large, about 13 pc in radius, with low surface brightness, well-developed "elephant trunks," and a hole in the center. It is impinging upon surrounding dark clouds, producing bright rims.

b) Region A, *the Site of an Older Subgroup in* Cep OB 2

In certain ways, the appearance of Region A resembles that of the region of Cep OB3 in the interior of the H I ring. It is true no expansion velocities, particularly any peculiar "forbidden" velocities are observed in its direction. However, there are features of the region that suggest an expansion of the H I as well as some ionization has taken place there.

Firstly, the region contains a large proportion of evolved massive stars such as μ Cep (M2 Ia), ν Cep (A2 Ia), 19 Cep (O 9.5 Ib) and VV Cep (M2ep Ib + B2pe). We suggest this part of the association forms a subgroup, Cep OB2a, whose age is about 10^7 yr. A younger subgroup, Cep OB2b, is the cluster Trumpler 37, whose earliest main sequence star is O6, thus with an age of about 4×10^6 yr. As is typical of associations, the older subgroup occupies a larger volume. This can be simply due to the velocity dispersion of the stars, which are not gravitationally bound.

Secondly, at least one "runaway star" is present in Region A, λ Cep, at $V = +61\,\mathrm{km\,s^{-1}}$. Blaauw (1961) also attributes the runaway star 68 Cyg to Cep OB2. So probably at least one supernova has exploded there, as this process is believed to produce the runaway stars.

No remnant has been detected, but no supernova remnants older than 10^6 yr are known (Ilovaisky and Lequeux, 1972).

Thirdly, the dust in the region takes the form of dense, small, filamentary wisps, particularly Kh 173, 169, 172 and 177. Van den Bergh (1972) has called this part of the region a "fossil H II region." He considers these structures left over from an extinct H II region whose exciting stars no longer shine.

Together, these characteristics suggest that in the recent past, $\sim 10^7$ years ago, Region A was an active site of star formation. The stars produced here have since spread over a large volume due to their velocity dispersion. Many have evolved into supergiants, some into supernovae. There was at least one H II region present during part of the time.

Presumably there had to be an abundance of dense gas in order to form the stars and fuel the H II region. For the region to appear empty of H I emission as it does, there are three possibilities: the gas has expanded away, it is opaque and cold, or it is ionized. The gas may well have expanded away, but it is hard to conceive that it occupies a much larger volume than the association, within a factor two or so. It is unlikely to be cold and opaque, because the region is clear of dust, except for those few filamentary clouds.

As for ionization, the large-scale Hα survey of Sivan (1974) reveals diffuse Hα emission exactly in Region A. It extends between $\ell \approx 102°$ and 106°, $b \approx -1°$ to 49°. This emission is just barely discernible on the POSS prints. Johnson (1965) estimates the minimum emission measure, $E = \int n_e^2 \, dR$, visible on POSS red prints is 400–600 cm^{-6} pc, while Poveda (1963) estimates the minimum $E = 50$ cm^{-6} pc. If we take $R = 830$ pc, with the depth the mean of the orthogonal dimensions, we find the value of the ionization parameter to be $U = 110$ cm^{-2} pc for $E = 500$ cm^{-6} pc and $U = 50$ cm^{-2} pc for $E = 50$ cm^{-6} pc.

Adding the contributions of the early-type stars in the region as shown in Fig. 3(d) and using the calibration of Churchwell and Walmsley (1973), the ionization parameter based on stars is in the range $U \approx 120$–160 pc cm^{-2}.

The agreement between the ionization parameter from Hα emission and that from early-type stars shows that very likely practically all the gas present is ionized.

9. Conclusions and Discussion

a) The Association at 800 pc

Two concentrations of H I and a region of ionized gas were found in the vicinity of Cep OB2 and Cep OB3, at ~ 800 pc from the sun.

A large H I shell, coinciding with a prominent ring of dark clouds 8° in diameter, surrounds Cep OB3. The shell appears to be expanding at ~ 10 km s^{-1}. Its mass is $5.3 \times 10^4 \mathscr{M}_\odot$, and the kinetic energy of expansion is 5×10^{49} erg.

From a study of H I absorption features, CTB 107 and S 154 are found to be present in the complex consisting also of Cep OB3 and its surrounding shell. Their radio continuum radiation indicates they contain on the order of 10 stars of spectral type O9.

Cep OB2 was found to consist of two subgroups of differing ages. Cep OB2a occupies the region $\ell = 100°$ to 106°, $b = +2°$ to $+8°$, and contains many evolved massive stars. The region appears low in H I emission, but Hα photographs show it to be significantly ionized, in good agreement with the uv output of the stars. Cep OB 2b consists of Tr 37 in IC 1396. It is surrounded by an H I concentration of $2 \times 10^4 \mathscr{M}_\odot$ that correlates in outline with the bright-rimmed dark clouds adjoining the H II region.

Cep OB2 and OB3 together form a complex of star formation sites—clusters, dispersing associations, and interstellar clouds. Cep OB3 has a somewhat different character than Cep OB2, and we don't propose to lump them together as parts of the same association. They lie close together, however, and they may even be interacting. Cep OB3, more compact than Cep OB2, seems isolated within its surrounding shell of dust and gas. The separation between the older and younger subgroups of Cep OB2 is about the same as the distance between the older subgroup and Cep OB3. The dark cloud Kh 187 prevents us from seeing stars that might make the connection more evident, but we know such stars are there in CTB 107 and S 154. The overall size of the entire complex is about 140 × 90 pc. It probably also extends to Cep OB4 (cf. Alter *et al.*, 1970).

We can identify five sub-associations of different ages in the complex: Cep OB2a, 7×10^6 yr; Cep OB2b or Tr 37, 3×10^6 yr; Cep OB3a, 8×10^6 yr; Cep OB3b, 4×10^6 yr, and CTB 107, whose age is unknown but probably 2–4×10^6 yr.

The interstellar matter in the complex is in a dynamic state of expansion. In the younger subgroups we see it as ionized gas impinging upon bright-rimmed dark clouds that contain neutral gas, e.g., in IC 1396. In the older subgroups, we see an expanding shell in Cep OB3 and a low-density, partially ionized region with a fossil H II region and relics of supernova explosions in Cep OB2a.

Based on the observations, regions where hot stars form appear to get swept clear of gas by the heat and explosions of the stars on a time scale shorter than the stellar lifetime. At sufficiently low densities, much of the hydrogen is also ionized. This probably explains the lack of H I in clusters found by Gordon *et al.* (1968). The present case is one of the few instances where the Hα has been actually observed.

There are indications of direct interactions among the subgroups, raising questions we are as yet unable to answer. The sharp boundary of the H I concentration around Tr 37 faces the ionized region of Cep OB 2a. Could the expansion of the gas in Cep OB 2a have provided the extra pressure needed to collapse the cloud that eventually formed Tr 37? Is CTB 107 the result of a similar process occurring on the boundary of the Cep OB 3 shell?

b) The Gas at 400 pc—*a Galactic Shock Front?*

Three concentrations, denoted Regions I, III and IV, were found at 400 pc from the sun. Kh 141 in Region I contains cool H I with $T_s < 40$ K that coincides with a line of small, opaque dust clouds in its center. Region III contains about 900 $\mathcal{M}_\odot$ of H I near S 129. Region IV corresponds to Cep R 2. It contains several Orion-population variables. Feature *U* in Region *V* also appears to be connected with this gas. The H I mass in Region IV is about $7 \times 10^3 \mathcal{M}_\odot$. Its line-of-sight velocity, $V \approx -10$ km s^{-1}, is remarkable for being more negative than the main maximum, which contains gas associated with Cep OB 3 at twice the distance. (Much of the main maximum gas, however, is nearby.)

At higher longitudes, Region IV joins Heiles's (1967) "high-velocity sheet". In the maps of Weaver and Williams (1974b) and Burton and Verschuur (1973) the feature continues around to $\ell \approx 170°$ before becoming confused with the more distant gas whose velocity approaches zero there. Lindblad (1967) traced this feature through the anticenter direction, calling it his Feature *C* (not the H I feature he connects with Gould's Belt). It is prominent at $b = +4°$ and above, reaching to $b \gtrsim +15°$.

In Fig. 9(a), the outline of this positive-latitude feature is shown on the sky. For comparison with the dust distribution, which is hard to discern as individual dark clouds at these latitudes, the zone of avoidance from Steinlin (1962) is also shown. There seems to be a good correlation.

Figure 9(b) shows the ℓ, V diagram of the peak velocity of the feature. Occasionally the feature tends to split into two components at different latitude and velocity. This is indicated by the dot and cross symbols.

The continuity in $T_b(\ell, b, V)$ coordinates suggests we are viewing some sort of cohesive structure. The high mean latitude and the wide latitude width, together with the photometric distance $R = 400$ pc to Cep *R* 2 at $\ell = 110°$, indicate the structure is nearby. Its velocity is therefore non-circular.

Because of symmetry about $\ell = 135°$ in Fig. 9(b), the peculiar velocity must be mostly along a galactic radius. The velocity pattern can be reasonably well matched by a segment of a spiral inclined at a pitch angle of $i = 15°$ to 25°, passing through the point $\ell = 110°$, $R = 400$ pc, and having an inward velocity of 10 km s^{-1} along a galactic radius. This is shown in Fig. 9(b).

In the theory of spiral density waves (e.g., Shu *et al.*, 1972), this sort of structure could be interpreted as a line of clouds that has recently passed through a galactic shock. (The structure is so localized that we observe primarily density effects; velocity crowding makes only a small difference.) The appearance of the dust associated with the H I tends to bear this out—numerous highly condensed cores, often associated with Orion-population variables, within a more amorphous envelope.

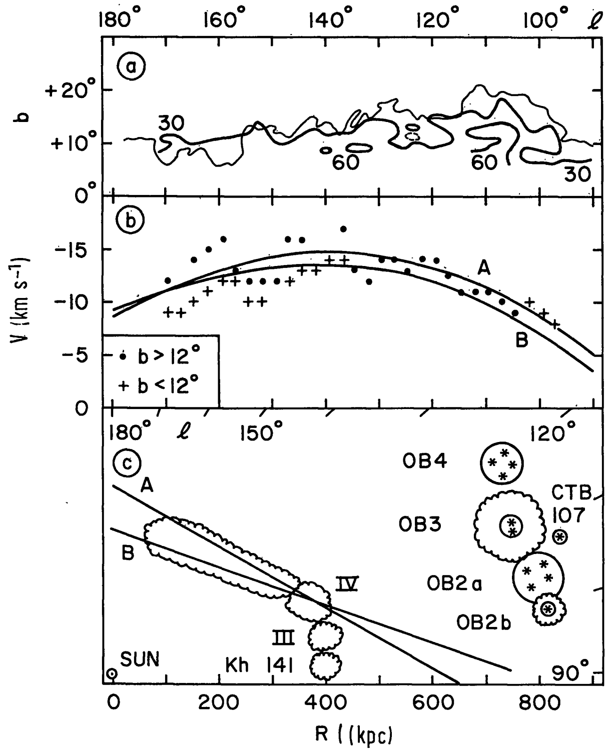

Fig. 9. (a) Outline of $T_a = 30$ K and $T_b = 60$ K contours (Weaver and Williams, 1974a) for the positive-latitude feature at $V \approx -10$ km s^{-1} (heavy lines), compared with contour of 4 galaxies per deg^2 from Steinlin (1962). (b) $T_b(\ell, V)$ diagram for central velocity of the positive-latitude feature from Weaver and Williams (1974b), compared with ℓ, *V* diagrams for spirals *A* and *B*, with pitch angles 15° and 25°, passing $\ell = 110°$ at $R = 400$ pc, with inward velocity of 10 km s^{-1}. (c) Schematic diagram of the region showing OB associations near $R = 800$ pc and a line of dark clouds at $R \approx 400$ pc.

c) The Pattern of Star Formation in the Solar Vicinity

A schematic diagram of the area is shown in Fig. 9(c). The pattern suggests we may be witnessing the propagation of a spiral shock in this region of Cepheus. Lines A and B give the spiral pattern for the positive-latitude line of clouds, which connects with Region IV, probably Region III, and possibly with Kh 141. Some of these clouds are high condensed. Star formation is occurring there now, producing Orion-population variables and clusters of infrared stars.

At some distance behind this line of dark clouds and H I concentration lies the complex consisting of Cep OB 2, Cep OB 3, CTB 107 and probably also Cep OB 4. Here the formation of massive stars has been in progress for

10^7 years. The segregation of ages with angle around the galactic center is much the same as that used to justify the density-wave theory. However, this view does not include the whole panorama of star formation in the solar vicinity. On the other side of the sun lies the Sco-Cen association, which repeats the pattern of condensed clouds associated with cool H I with peculiar inward motion, Orion-population variables, infrared clusters, and OB association sub-groups of ages exceeding 10^7 yr. In addition, Lindblad *et al.* (1973) show that the H I gas very near the sun shows a peculiar *outward* motion in the anticenter direction (which they interpret as part of an expanding gaseous disk).

This confused pattern—star formation over lengthy periods in small regions, non-circular motions of opposite signs, spiral alignments of H I concentrations, and dust clouds of various morphology—can hardly be interpreted as a single dust lane marking a galactic shock followed by newly formed stars of increasing age. It is clear, however, that formation of massive stars, once started in a region, proceeds in spurts for a long time. This has been known almost since the first recognition of stellar associations. In Cepheus we find indications that the expansion of the gas in a subgroup may trigger collapse of neighboring clouds. The process may run on like a string of firecrackers through a cloud complex, branching off in several directions. As Baade (1963) remarked, "when star formation is going on in an area it spreads in some way like a disease."

Acknowledgements. The observations were supported by the Netherlands Organization for Advancement of Pure Research (Z.W.O.). Partial support for S.C.S. was provided by the U.S. National Science Foundation.

References

Alter, G., Balázs, B., Vanysek, V. 1970, Catalogue of Star Clusters and Associations, Budapest, Akadémiai Kiadó, p. 2447

Baade, W. 1963, Evolution of Stars and Galaxies, Harvard Univ. Press, Cambridge, p. 224

Berkhuijsen, E.M. 1972, *Astron. & Astrophys. Suppl. Ser.* **5**, 263

Blaauw, A. 1961, *Bull. Astron. Inst. Neth.*, **15**, 265

Blaauw, A. 1963, The Calibration of Luminosity Criteria in *Basic Astronomical Data*, Ed. K. Aa. Strand, Univ. Chicago Press, Chicago, p. 383

Blaauw, A. 1964, *Ann. Rev. Astron. & Astrophys.* **2**, 213

Blanco, V.M., Demers, S., Douglass, G.G., FitzGerald, M.P. 1968, *Publ. U.S. Naval Obs.* **21**, 1

Burton, W.B. 1970, *Astron. & Astrophys. Suppl. Ser.* **2**, 261

Burton, W.B., Verschuur, G. 1973, *Astron. & Astrophys. Suppl. Ser.* **12**, 145

Churchwell, E., Walmsley, C.M. 1973, *Astron. & Astrophys.* **23**, 117

Felli, M., Churchwell, E. 1972, *Astron. & Astrophys. Suppl. Ser.* **5**, 369

FitzGerald, M.P. 1970, *Astron. & Astrophys.* **4**, 234

Garrison, R.F. 1970, *Astron. J.* **75**, 1001

Garmany, O.D. 1973, *Astron. J.* **78**, 185

Girstein, H.-G., Rohlfs, K. 1964, *Z. Astrophys.* **59**, 83

Gordon, C.P., Howard, W.E., III, Westerhout, G. 1968, *Astrophys. J.* **154**, 103

Grasdalen, G.L., Kuhi, L.V., Harlan, E.A. 1973, *Publ. Astron. Soc. Pacific* **85**, 193

Harten, R.H., Westerhout, G., Kerr, F.J. 1975, *Astron. J.* **80**, 307

Heiles, C. 1967, *Astrophys. J. Suppl. Ser.* **15**, 97

Herbig, G.H., Rao, N.K. 1972, *Astrophys. J.* **174**, 401

Howard, W.E., III. 1958, *Astron. J.* **63**, 50

Ilovaisky, S.A., Lequeux, J. 1972, *Astron. & Astrophys.* **20**, 347

Johnson, H.M. 1965, Diffuse Nebulae in *Nebulae and Interstellar Matter*, Ed. B.M. Middlehurst and L.H. Aller, Univ. Chicago Press, Chicago, p. 65

Kerr, F.J. 1965, Radio-line emission and absorptions by the interstellar gas in *Nebulae and Interstellar Matter*, Ed. B.M. Middlehurst and L.H. Aller, Univ. of Chicago Press, Chicago, p. 575

Kerr, F.J., Knapp, G.R. 1974, *Astron. & Astrophys.* **35**, 361

Khavtassi, J. 1960, Atlas of Galactic Dark Nebulae, Abastumani Astrophys. Obs.

Knapp, G.R. 1972, unpublished Ph. D. thesis, Univ. of Maryland, College Park.

Lindblad, P.O. 1967, *Bull. Astron. Inst. Neth.* **19**, 34

Lindblad, P.O., Grape, K., Sandqvist, Aa., Schober, J. 1973, *Astron. & Astrophys.* **24**, 309

Lynds, B.T. 1962, *Astrophys. J. Suppl. Ser.* **7**, 1

Menon, T.K. 1958, *Astrophys. J.* **127**, 28

Pottasch, S.R. 1965, *Vistas* **6**, 149

Poveda, A. 1963, *Bol. Obs. Tonantzintla y Tacubaya* **3**, 119

Racine, R. 1968, *Astron. J.* **73**, 233

Sancisi, R. 1974, IAU *Symposium No.* **60**, p. 115

Schmidt, M. 1965, Rotation parameters and distribution of mass in the Galaxy in *Galactic Structure*, Ed. A. Blaauw and M. Schmidt, Univ. Chicago Press, Chicago, p. 513

Sharpless, S. 1959, *Astrophys. J. Suppl. Ser.* **4**, 257

Shu, F.H., Milione, V., Gebel, W., Yuan, C., Goldsmith, D.W., Roberts, W.W. 1972, *Astrophy. J.* **173**, 557

Simonson, S.C., III 1968, *Astrophys. J.* **154**, 923

Simonson, S.C. III 1974, IAU *Symposium No.* **52**, p. 227

Sivan, J.P. 1974, *Astron. & Astrophys. Suppl. Ser.* **16**, 163

Steinlin, U.W. 1962, *Astron. J.* **67**, 370

Strom, S.E., Strom, K.M., Yost, J., Carrasco, L., Grasdalen, G. 1972, *Astrophys. J.* **173**, 353

Van den Bergh, S. 1972, *Vistas* **13**, 265

Weaver, H., Ebert, A. 1964, *Publ. Astron. Soc. Pacific* **76**, 6

Weaver, H., Williams, D.R.W. 1973, *Astron. & Astrophys. Suppl. Ser.* **8**, 1

Weaver, H., Williams, D.R.W. 1974a, *Astron. & Astrophys. Suppl. Ser.* **17**, 1

Weaver, H., Williams, D.R.W. 1974b, *Astron.& Astrophys. Suppl. Ser.* **17**, 251

Westerhout, G. 1957, *Bull. Astron. Inst. Neth.* **13**, 201

Westerhout, G. 1973, Maryland-Green Bank Galactic 21-cm Survey, 3rd Ed. (preprint)

Williams, D.R.W. 1973, *Astron. & Astrophys. Suppl. Ser.* **8**, 505

S. Christian Simonson, III
3 Empire Place
Greenbelt, MD 20770, USA

H.W. van Someren Greve
Radiosterrenwacht Dwingeloo
Dwingeloo, The Netherlands